Accepted Manuscript

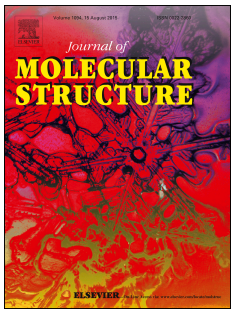

Novel pyrrole derivatives bearing sulfonamide groups: Synthesis *in vitro* cytotoxicity evaluation, molecular docking and DFT study

Masoumeh Bavadi, Khodabakhsh Niknam, Omolbanin Shahraki

PII: S0022-2860(17)30778-0

DOI: 10.1016/j.molstruc.2017.06.003

Reference: MOLSTR 23886

To appear in: *Journal of Molecular Structure*

Received Date: 1 March 2017

Revised Date: 4 May 2017

Accepted Date: 1 June 2017

Please cite this article as: M. Bavadi, K. Niknam, O. Shahraki, Novel pyrrole derivatives bearing sulfonamide groups: Synthesis *in vitro* cytotoxicity evaluation, molecular docking and DFT study, *Journal of Molecular Structure* (2017), doi: 10.1016/j.molstruc.2017.06.003.

Novel Pyrrole Derivatives bearing Sulfonamide Groups: Synthesis, *In Vitro* Cytotoxicity Evaluation, Molecular Docking and DFT Study

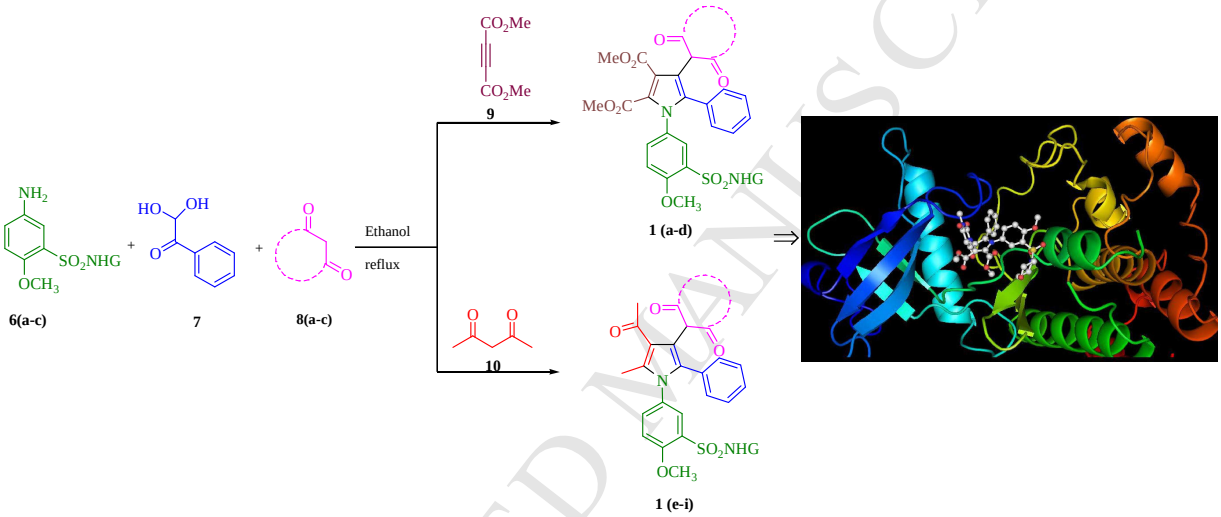

Novel pyrrole derivatives bearing sulfonamide groups: Synthesis *in vitro* cytotoxicity evaluation, molecular docking and DFT study

Masoumeh Bavadi, *[,a] Khodabakhsh Niknam[a] and Omolbanin Shahraki,[b]

[a]Department of Chemistry, Faculty of Sciences, Persian Gulf University, Bushehr, 75169 Iran; E-mail: mbavadi@gmail.com

[b] Department of Medicinal Chemistry, Faculty of Pharmacy, Zahedan University of Medical Sciences, Zahedan, Iran

Abstract

The synthesis of new derivatives of pyrrole substituted sulfonamide groups is described. The *in vitro* anticancer activity of these pyrroles was evaluated against MCF7, MOLT-4 and HL-60 cells using MTT assay. The target compounds showed inhibitory activity against tested cell lines. Among the compounds, compound **1a** exhibited good cytotoxic activity. The potential of this analog to induce apoptosis was confirmed in a nuclear morphological assay by Hoechst 33258 staining in the PC-12 cells. Finally, molecular docking was performed to determine the probable binding mode of the designed pyrrole derivatives into the active site of FGFR1 protein. DFT calculations were carried out at the B3LYP levels of theory with 6-31+G (d,p) basis set for compound **1a**. The point group (C_1) of it was obtained based on the optimized structures; the calculation of the FT-IR vibrational frequencies, ^{1}H NMR and ^{13}C NMR chemical shifts of the compound were carried out and compared with those obtained experimentally.

Keywords: Pyrrole, Anticancer, Sulfonamide, MTT, Molecular docking, DFT

1. Introduction

These days the number of cancer related mortality is increasing and one of the most leading causes of death in the world is cancer. Despite the immense advances and efforts in the field of cancer research, no currently available drugs can exterminate cancer cells without harming normal tissues [1]. The fibroblast growth factor (FGF) that signals through FGF receptors (FGFR1, FGFR2, FGFR3 and FGFR4) plays an important role in many physiologic processes, comprising embryogenesis, regulation of angiogenesis, wound healing and inflammation [2-4]. These families of proteins are expressed on various types of cells and regulate cellular actions, such as proliferation, differentiation, survival and metastasis of tumor cells. In this view, they are considered as the targets for cancer therapy [5].

There are several reports on small molecule FGFR inhibitors. Some of them such as **NVP-BGJ398** and **AZD4547** have entered clinical trials and **LY2874455** showed good FGFR inhibitory activity [6] (Fig. 1). Different series of nitrogen containing five-membered heterocyclic compounds have been reported as inhibitors of FGFR [7-9]. Therefore, the development and discovery of new anticancer agents with promising activity, selective and high therapeutic index is still a major challenge to medicinal chemists.

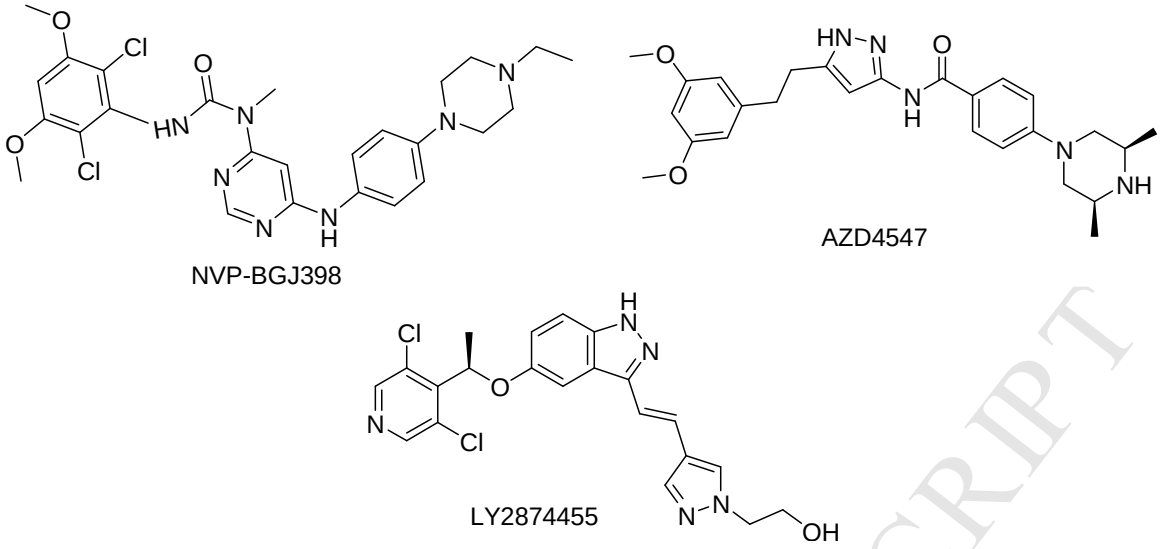

Fig. 1. The structure of some FGFR inhibitors.

Pyrrole and its derivatives are well known as the most important nitrogen-containing heterocyclic compounds due to their present as structural subunits of many natural products including heme, vitamin B12, and cytochromes, bile pigments, and alkaloids [10, 11].

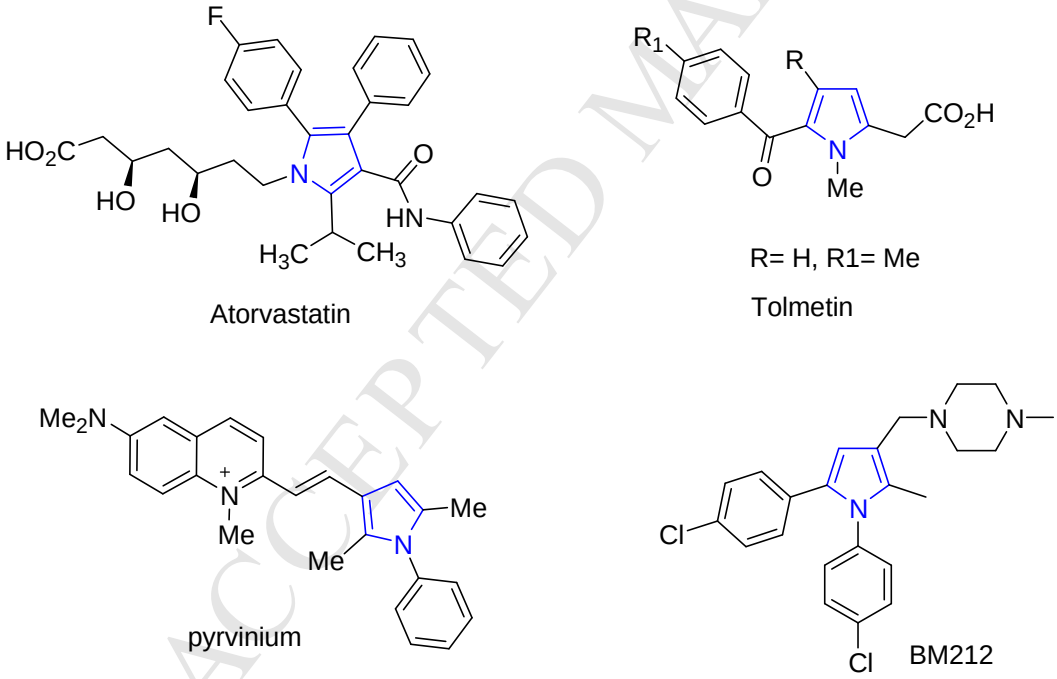

Fig. 2. The biologically active compounds containing the pyrrole moiety.

They have also exhibited remarkable biological activities such as antibacterial [12], antitubercular [13], antitumor [14], anti-inflammatory [15] and antioxidant activity [16]. Some biologically important compounds containing the pyrrole moiety such as atorvastatin (a cholesterol-lowering agent), tolmetin and anthelmintic pyrvinium (nonsteroidal anti-inflammatory drugs), BM212 and its derivatives (Mycobacterium

tuberculosis activity) [17-21] are shown in Fig. 2. Moreover, pyrroles are used as insecticides [22] and useful building units in the field of material chemistry [23].

In recent years, the synthesis of drugs bearing sulfonamide groups in their structures has been attended. They are exhibited a significant biological properties including anticancer [24], antimalarial [25], anti-inflammatory [26], antihypertensive [27], anticonvulsant, and herbicidal properties [28]. A series of these drugs such as sulfonamide KCN1 which was reported as an antitumor agent and the HIV protease inhibitor amprenavir was used for the treatment of AIDS and HIV infections [29, 30]. In addition, it was reported that sulfonamides were used as inhibitors of the activity of the enzymes for example; dihydropteroate synthase (DHPS) [31], matrix metalloproteinase [32], and carbonic anhydrase (CA) [33].

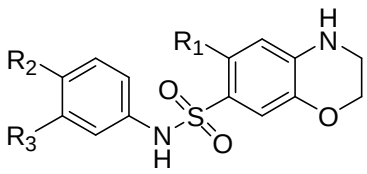

benzoxazine-6-sulfonamides

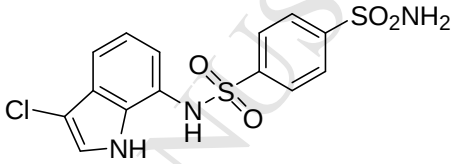

E7070

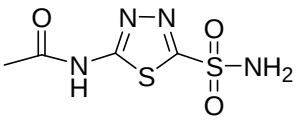

AZA

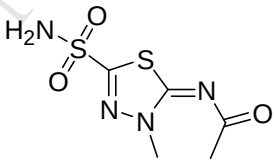

MZA

Fig. 3. Chemical structures of some therapeutic sulfonamides.

Moreover, sulfonamide drugs have been reported such as benzoxazine-6-sulfonamides and **E7070** (anticancer agents) [34, 35], and anti-glaucoma compounds acetazolamide **AZA** and methazolamide **MZA** [36-38] (Fig. 3). Therefore, due to the pharmacological and biological importance of sulfonamides and nitrogen-containing heterocyclic compounds in medicinal chemistry, the synthesis of compounds bearing sulfonamide moieties with the aim of outstanding biological properties has become interesting field in research.

In this study, we reported the synthesis of a new class of pyrrole derivatives substituted sulfonamide groups. These compounds were subsequently evaluated for anticancer activity and

morphological study. The binding mode of these derivatives with the active site of the FGFR1 protein was also investigated by molecular docking.

2. Experimental Section

2.1. Materials and methods

The chemicals were purchased from Merck and Aldrich Chemical Companies. The progress of the reactions was monitored by TLC on silica gel PolyGram SILG/UV254 plates. For recorded ^{1}HNMR and ^{13}C NMR (400 MHZ and 100 MHZ, respectively) spectra we used Bruker (400 MHz) Avance Ultrashield in pure deuterated DMSO-d_6 solvent with tetramethylsilane (TMS) as internal standards. The FT-IR spectroscopy (Shimadzu FT-IR 8300 spectrophotometer) was run for characterization of the products. Mass spectra (FINNIGAN-MAT 8430 mass spectrometer) were employed at 70 eV. Melting points were obtained in open capillary tubes in a Barnstead Electrothermal 9100 BZ circulating oil melting point apparatus. PC-12 (rat pheochromocytoma), MCF7 (human breast adenocarcinoma), MOLT-4 (human acute lymphoblastic leukemia) and HL-60 (promyelocytic leukemia) cells were obtained from the National Cell Bank of Iran Pasteur Institute (Tehran, Iran). The cell culture medium (RPMI 1640), fetal bovine serum (FBS), and penicillin–streptomycin were obtained from Gibco BRL (Life technology, Paisley, Scotland). 3-(4,5-Dimethyltiazol-2-yl)-2,5-diphenyl-tetrazolium bromide (MTT) powder and Hoechst 33258 were purchased from Sigma Chemicals Co. (Germany). The culture plates were purchased from Nunc (Denmark).

2.2 Cytotoxicity activities

2.2.1. Cell culture

All cell lines were cultured in RPMI 1640 medium supplemented with 10% fetal bovine serum, 100 µg/mL streptomycin, and 100 U/mL penicillin at 37 ^{o}C in a humidified incubator with 5% CO_2.

2.2.2. Cytotoxicity assay

The cytotoxicity activity of the synthesized compounds was determined by 3-(4,5-dimethylthiazol-2-yl)-2,5-diphenyl-tetrazolium bromide (MTT) assay. The cells were seeded in 96-well plates (5×10^4 cells/mL) and incubated for 24 h to allow cell attachment. In order to prepare stock solution, all of the synthesized compounds were dissolved in DMSO. The final concentration of DMSO in the culture medium did not exceed 0.5%. Different concentrations of the compounds (25, 50, 100 and 200 µM) were prepared in

culture medium and added to the wells in triplicate and incubated for another 72 h. In the following, 800 µL of MTT reagent (5 mg/mL) was diluted in 5.6 mL phosphate buffered serum (PBS). 80 µL of the obtained MTT solution was added to each well and the plates incubated for an additional 3 h at 37 ^{o}C. Thereafter, the culture medium was removed and the formazan precipitates were dissolved in 200 µL dimethylsulfoxide (DMSO). Cisplatin was used as a positive control. Finally, the absorbance of each well was determined by plate reader (Anthous 2020; Austria) at 570 nm with background correction at 655 nm. Cell viability was calculated using the following formula:

$$Viability = \frac{Ab(S) - Ab(B)}{Abs(C) - Ab(B)} \qquad (1)$$

Where Ab (S), Ab (B) and Ab (C) are the colorimetric intensity of the cells incubated with the samples, blank (wells contained only growth medium for background correction) and negative control (wells contained cells but no drugs) respectively. IC_{50} values were calculated with the software CurveExpert version 1.34 for Windows.

2.2.3. Morphological study

PC-12 cells (5 ×10^3/well) were seeded in 24-well plates and incubated for 24 h. The cells were treated with and without compound **1a** for 48 h. After incubation, the cell morphology was assessed by Axiovert 25 phase-contrast microscope (Zeiss, Germany).

2.2.4. Hoechst 33258 staining Assay

The ability of the target compounds to induce apoptosis in PC-12 cells was evaluated morphologically by Hoechst 33258 staining test [39]. Briefly, the cells (7 × 10^4/well) were seeded in 12-well plates and incubated in a humidified atmosphere at 37 ^{o}C with 5% CO_2. Then, the cells were treated with and without compound **1a** for 48 h. Plates were washed with PBS and stained with 0.5 µL of Hoechst 33258 (10 mg/mL) and incubated at 37 ^{o}C for 15 min at room temperature. Afterwards, the cells were immediately analyzed by an Axoscope2 plus fluorescence microscope from Zeiss (Germany).

2.3. **Molecular docking**

The crystal structure of FGFR1 was obtained from the Protein Data Bank (PDB code: 4ZSA). Water molecules and co-crystalized ligands were excluded. Validation of molecular docking protocol was checked via testing the ability of AUTODOCK 4.2 to reproduce the binding mode of cognate ligand. The PDB file

of protein was regenerated. An N-terminus of a chain is capped with ACE (acetyl) while C-terminus is capped with NME (formyl) moiety. The Reduce program [40] used to determine the hydrogen coordinates using steric considerations and geometric hydrogen bond network analysis; ionization and flipped states of His, Glu and Asp are assigned on geometric grounds alone and rotamers are assigned from a fixed discrete collection. The loops were modeled by MODELLER 9v2 program [41] by merging the appropriate residues in missing loop locations. The three-dimensional structures of compounds were built using the Avogadro software. Structure optimization at [B3LYP combined to 6-31G (d,p) and 6-31+G(d,p)] level of theory was performed using Gaussian 09 package software. The degrees of torsions were defined to generate PDBQT format of the ligands. The grid parameter file was created using AutoGrid implemented in the MGLTools package. The grid size was set to 60 × 60 × 60 points with spacing value 0.375 A. The prepared ligands were docked in the rigid macromolecule using Lamarckian Genetic Algorithm (LGA), with 200 GA runs and 25000 000 energy evaluations while the other parameters were left as default.

Molecular docking was performed by AutoDock 4.2 and results were analyzed with the aid of the AutoDockTools-1.5.6. Cluster analysis was done on the docking results using a Root mean square deviation (RMSD ≤ 2 Å).

2.4. **General procedure for the synthesis of pyrrole derivatives bearing sulfonamide groups (1)**

A mixture of sulfonamide (**6**; 1 mmol), phenylglyoxal monohydrate (**7**; 1 mmol), 1,3-dicarbonyl compound (**8**; 1mmol), dimethyl acetylene dicarboxylate (**9**; 1 mmol) or acetylacetone (**10**; 1 mmol) in ethanol (96%, 5 mL) was refluxed with stirring in an oil bath. The progress of the reaction was monitored by TLC. After completion of the reaction, the resulting solids were filtered and washed with warm ethanol to obtain pure product [42].

Dimethyl-4-(1,3-dimethyl-2,4,6-trioxohexahydropyrimidin-5-yl)-1-(4-methoxy-3-(morpholinosulfonyl)phenyl)-5-phenyl-1*H*-pyrrole-2,3-dicarboxylate (**1a**): Light pink solid; Yield: 95%; m.p. 177-179 ^{o}C; IR (KBr) (ν_{max},cm^{-1}): 3000, 2980, 2850 (C–H), 1522 (C=C), 1729, 1678 (C=O), 1344, 1165 (SO_2); ^{1}H NMR (400 MHz, DMSO-d_6) δ (ppm): 2.78 (m, 4H, 2 × CH_2), 3.18 (s, 6H, 2 × CH_3), 3.52–3.54 (m, 4H, 2 × CH_2), 3.64 (s, 3H, CH_3), 3.69 (s, 3H, CH_3), 3.90 (s, 3H, OCH_3), 4.98 (s, 1H, CH), 7.20-7.22 (m, 2H, Ar), 7.30-7.36 (m, 5H, Ar), 7.68 (dd, 1H, J_1 = 8.8, J_2 = 2.8 Hz, Ar); ^{13}C NMR (100 MHz, DMSO-d_6) δ (ppm): 28.9, 46.1, 52.3, 53.3, 56.9, 66.1, 114.3, 116.0, 124.7, 128.4, 128.8, 128.9, 129.2, 129.3, 129.7, 130.7, 131.1, 134.8, 138.7, 152.1, 157.0, 162.0, 163.9, and 168.0; Mass spectrum *m/z*: 668.3 [M^{+}]; Anal. Calcd. (%) $C_{31}H_{32}N_4O_{11}S$: C, 55.68; H, 4.82; N, 8.38; S, 4.80; Found: C, 55.37; H, 4.79, N, 8.11; S, 4.48.

Dimethyl-4-(1,3-dimethyl-2,4,6-trioxohexahydropyrimidin-5-yl)-1-(4-methoxy-3-(*N*-phenylsulfamoyl)phenyl)-5-phenyl-1*H*-pyrrole-2,3-dicarboxylate (**1b**): Light pink solid; Yield: 96%,

m.p. 207-209 ^{o}C; IR (KBr) (ν_{max},cm^{-1}): 3288 (N–H), 3100 (C–H), 1495 (C=C), 1723, 1692 (C=O), 1332, 1158 (SO_2); ^{1}H NMR (400 MHz, DMSO-d_6) δ (ppm): 3.18 (s, 6H, 2 × CH_3), 3.56 (s, 3H, OCH_3), 3.63 (s, 3H, OCH_3), 3.89 (s, 3H, OCH_3), 4.97 (s, 1H, CH), 6.99-7.05 (m, 3H, Ar), 7.11-7.14 (m, 3H, Ar), 7.20-7.28 (m, 4H, Ar), 7.32-7.36 (m, 1H, Ar), 7.42 (dd, 1H, J_1 = 8.8, J_2 = 2.8 Hz, Ar), 7.57 (d, 1H, J = 2.8 Hz, Ar), 10.20 (s, 1H, SO_2NH); ^{13}C NMR (100 MHz, DMSO-d_6) δ (ppm): 28.9, 48.2, 52.3, 53.2, 57.1, 113.2, 113.8, 115.9, 119.8, 124.2, 126.8, 128.5, 128.7, 129.1, 129.4, 129.5, 129.9, 130.0, 130.3, 130.9, 134.8, 137.8, 138.6, 152.2, 156.6, 161.9, 163.8, and 168.0; Mass spectrum *m/z*: 674.3 [M^{+}]; Anal. Calcd. (%) $C_{33}H_{30}N_4O_{10}S$: C, 58.75; H, 4.48; N, 8.30; S, 4.75; Found: C, 58.43; H, 4.51, N, 7.98; S, 4.46.

Dimethyl-1-(3-(*N*-(chlorophenyl)sulfamoyl)-4-methoxyphenyl)-4-(1,3-dimethyl-2,4,6-trioxohexahydropyrimidin-5-yl)-5-phenyl-1*H*-pyrrole-2,3-dicarboxylate (**1c**): Light pink solid; Yield: 93%; m.p. > 250 ^{o}C; IR (KBr) (ν_{max},cm^{-1}): 3288 (N–H), 3050 (C–H), 1517 (C=C), 1722, 1691 (C=O), 1322, 1160 (SO_2); ^{1}H NMR (400 MHz, DMSO-d_6) δ (ppm): 3.18 (s, 6H, 2 × CH_3), 3.59 (s, 3H, CH_3), 3.63 (s, 3H, CH_3), 3.89 (s, 3H, OCH_3), 4.97 (s, 1H, CH), 7.01-7.04 (m, 1H, Ar), 7.11-7.14 (m, 3H, Ar), 7.24-7.33 (m, 6H, Ar), 7.44 (dd, 1H, J_1 = 8.8, J_2 = 2.8 Hz, Ar), 7.56 (d, 1H, J = 2.8 Hz, Ar), 10.36 (s, 1H, SO_2NH); ^{13}C NMR (100 MHz, DMSO-d_6) δ (ppm): 28.9, 48.2, 52.3, 53.2, 57.1, 113.8, 115.9, 121.4, 126.2, 128.3, 128.5, 128.7, 129.0, 129.3, 129.5, 129.9, 130.0, 130.9, 135.0, 136.8, 138.6, 152.2, 156.6, 161.9, 163.8, and 168.0; Mass spectrum *m/z*: 710.3 [M^{+2}], 708.3 [M^{+}]; Anal. Calcd. (%) $C_{33}H_{29}ClN_4O_{10}S$: C, 55.89; H, 4.12; Cl, 5.00; N, 7.90; S, 4.52; Found: C, 55.61; H, 4.15, N, 7.57; S, 4.18.

Dimethyl-1-(3-(*N*-(4-chlorophenyl)sulfamoyl)-4-methoxyphenyl)-5-phenyl-4-(2,4,6-trioxohexahydropyrimidin-5-yl)-1*H*-pyrrole-2,3-dicarboxlate (**1d**): White solid; Yield: 88%; m.p. > 250 ^{o}C; IR (KBr) (ν_{max},cm^{-1}): 3241, 3184 (N–H), 3075 (C–H), 1538 (C=C), 1750, 1710 (C=O), 1342, 1161 (SO_2); ^{1}H NMR (400 MHz, DMSO-d_6) δ (ppm): 3.59 (s, 3H, CH_3), 3.67 (s, 3H, CH_3), 3.89 (s, 3H, OCH_3), 4.82 (s, 1H, CH), 6.91–6.93 (m, 1H, Ar), 7.01–7.03 (m, 1H, Ar), 7.10–7.14 (m, 3H, Ar), 7.22–7.35 (m, 5H, Ar), 7.42 (dd, 1H, J_1 = 9.0, J_2 = 2.4 Hz, Ar), 7.54 (d, 1H, J = 2.4 Hz, Ar), 10.36 (s, 1H, SO_2NH), 11.31 (s, 2H, NH); ^{13}C NMR (100 MHz, DMSO-d_6) δ (ppm): 48.1, 52.1, 53.2, 57.1, 113.8, 115.6, 121.4, 126.1, 128.2, 128.3, 128.5, 128.8, 128.9, 129.2, 129.4, 129.5, 129.9, 130.0, 130.1, 130.3, 130.9, 135.0, 136.8, 151.4, 156.6, 162.0, 163.8, and 169.6; Mass spectrum *m/z*: 682.7 [M^{+2}], 680.9 [M^{+}]; Anal. Calcd. (%) $C_{31}H_{25}ClN_4O_{10}S$: C, 54.67; H, 3.70; Cl, 5.21; N, 8.23; S, 4.71; Found: C, 54.34; H, 3.64, N, 7.91; S, 4.43.

5-(3-Acetyl-4-(1,3-dimethyl-2,4,6-trioxohexahydropyrimidin-5-yl)-2-methyl-5-phenyl-1*H*-pyrrol-1-yl)-2-methoxy-*N*-phenyl-benzenesulfonamide (**1e**): White solid; Yield: 94%; m.p. > 250 ^{o}C; IR (KBr) (ν_{max},cm^{-1}): 3419 (O–H, N–H), 3072 (C–H), 1573 (C=C), 1670 (C=O), 1346, 1159 (SO_2); ^{1}H NMR (400 MHz, DMSO-d_6) δ (ppm): 2.13 (s, 3H, CH_3), 2.16 (s, 3H, CH_3), 3.05 (s, 6H, CH_3), 3.89 (s, 3H, OCH_3), 6.95-6.99 (m, 5H, Ar), 7.00-7.03 (m, 3H, Ar), 7.14 (d, 1H, J = 8.8 Hz, Ar), 7.19-7.25 (m, 3H, Ar), 7.44 (d, 1H, J = 2.8 Hz, Ar), 10.16 (s, 1H, SO_2NH); ^{13}C NMR (100 MHz, DMSO-d_6) δ (ppm): 13.5, 27.6, 29.3, 57.0, 82.2, 113.8, 119.7, 120.1, 123.7, 124.1, 126.2, 126.5, 127.6, 129.5, 130.2, 130.5, 130.5, 132.8, 133.1, 134.9, 135.1, 138.0, 153.6, 155.8, 162.7, and 196.8; Mass spectrum *m/z*: 614.4 [M^{+}]; Anal. Calcd. (%) $C_{32}H_{30}N_4O_7S$: C, 62.53; H, 4.92; N, 9.11; S, 5.22; Found: C, 62.24; H, 4.88, N, 8.82; S, 4.89.

^{1}H NMR (400 MHz, DMSO-d_6 + D_2O) δ (ppm): 2.11 (s, 3H, CH_3), 2.15 (s, 3H, CH_3), 3.05 (s, 6H, CH_3), 3.87 (s, 3H, OCH_3), 6.95-6.96 (m, 4H, Ar), 6.98-7.04 (m, 4H, Ar), 7.12 (d, 1H, J = 8.8 Hz, Ar), 7.19-7.28 (m, 3H, Ar), 7.45(d, 1H, J = 2.4 Hz, Ar).

5-(3-Acetyl-4-(1,3-dimethyl-2,4,6-trioxohexahydropyrimidin-5-yl)-2-methyl-5-phenyl-1*H*-pyrrol-1yl)-*N*-(4-chlorophenyl)-2-methoxybenzenesulfonamide (**1f**): White solid; Yield: 89%; m.p. > 250 ^{o}C; IR (KBr) (ν_{max},cm^{-1}): 3419 (O–H, N–H), 3070 (C–H), 1574 (C=C), 1667, 1646 (C=O), 1350, 1160 (SO_2); ^{1}H NMR (400 MHz, DMSO-d_6) δ (ppm): 2.15 (s, 3H, CH_3), 2.16 (s, 3H, CH_3), 3.05 (s, 6H, CH_3), 3.89 (s, 3H, OCH_3), 6.95-6.99 (m, 5H, Ar), 7.01-7.04 (m, 2H, Ar), 7.15 (d, 1H, *J* = 8.8 Hz, Ar), 7.25-7.29 (m, 3H, Ar), 7.42 (d, 1H, *J* = 2.4 Hz, Ar), 10.33 (brs, 1H, SO_2NH); ^{13}C NMR (100 MHz, DMSO-d_6) δ (ppm): 13.5, 27.6, 29.3, 57.0, 82.2, 113.8, 120.1, 121.4, 123.7, 126.2, 127.6, 128.0, 129.4, 130.2, 130.5, 130.5, 132.8, 133.1, 134.9, 135.2, 153.6, 155.8, 162.7, and 196.8; Mass spectrum *m/z*: 650.3 [M^{+2}], 648.3 [M^+]; Anal. Calcd. (%) $C_{32}H_{29}ClN_4O_7S$: C, 59.21; H, 4.50; Cl, 5.46; N, 8.63; S, 4.94; Found: C, 58.87; H, 4.45, N, 8.32; S, 4.63.

5-(3-Acetyl-4-(4-hydroxy-2-oxo-2*H*-chromen-3-yl)-2-methyl-5-phenyl-1*H*-pyrrol-1-yl)-2-methoxy-*N*-phenylbenzenesulfonamide (**1g**): White solid; Yield: 83%; m.p. 219–221 ^{o}C; IR (KBr) (ν_{max},cm^{-1}): 3419 (O–H, N–H), 3080 (C–H), 1495 (C=C), 1635, 1600 (C=O), 1342, 1158 (SO_2); ^{1}H NMR (400 MHz, DMSO-d_6) δ (ppm): 2.16 (s, 3H, CH_3), 2.17 (s, 3H, CH_3), 3.89 (s, 3H, OCH_3), 6.96 (m, 5H, Ar), 7.01-7.04 (m, 3H, Ar), 7.09-7.16 (m, 3H, Ar), 7.19-7.23 (m, 2H, Ar), 7.33-7.37 (m, 2H, Ar), 7.49 (s, 1H, Ar), 7.80 (d, 1H, *J* = 7.2 Hz, Ar), 10.18 (s, 1H, SO_2NH); ^{13}C NMR (100 MHz, DMSO-d_6) δ (ppm): 13.5, 29.3, 57.0, 93.6, 113.9, 115.8, 119.7, 121.9, 124.1, 125.3, 126.4, 126.5, 127.7, 129.1, 129.5, 130.0, 130.1, 130.3, 130.5, 135.1, 138.0, 154.3, 155.9, 164.4, and 196.5; Mass spectrum *m/z*: 620.7 [M^+]; Anal. Calcd. (%) $C_{35}H_{28}N_2O_7S$: C, 67.73; H, 4.55; N, 4.51; S, 5.17; Found: C, 67.41; H, 4.52, N, 4.20; S, 4.87.

3-(4-Acetyl-1-(4-methoxy-3-(morpholinosulfonyl)phenyl)-5-methyl-2-phenyl-1*H*-pyrrol-3-yl)-4-hydroxy-2*H*-chromen-2-one (**1h**): White solid; Yield: 85%; m.p. 245–247 ^{o}C; IR (KBr) (ν_{max},cm^{-1}): 3419 (O–H), 3080 (C–H), 1496 (C=C), 1638, 1600 (C=O), 1343, 1161 (SO_2); ^{1}H NMR (400 MHz, DMSO-d_6) δ (ppm): 2.17 (s, 3H, CH_3), 2.37 (s, 3H, CH_3), 2.68–2.71 (m, 4H, 2 × CH_2), 3.53 (m, 4H, 2 × CH_2), 3.92 (s, 3H, OCH_3), 6.98–7.15 (m, 8H, Ar), 7.33–7.40 (m, 2H, Ar), 7.73–7.89 (m, 2H, Ar); ^{13}C NMR (100 MHz, DMSO-d_6) δ (ppm): 13.7, 29.3, 46.0, 56.9, 66.1, 93.3, 114.2, 115.8, 120.1, 122.0, 123.5, 124.6, 125.4, 126.3, 127.8, 130.0, 130.4, 130.6, 131.4, 132.5, 133.3, 135.1, 135.3, 154.3, 156.2, and 196.5; Mass spectrum *m/z*: 614.6 [M^+]; Anal. Calcd. (%) $C_{33}H_{30}N_2O_8S$: C, 64.48; H, 4.92; N, 4.56; S, 5.22; Found: C, 64.16; H, 4.87, N, 4.38; S, 4.91.

5-(3-Acetyl-2-methyl-5-phenyl-4-(2,4,6-trioxohexahydro-pyrimidin-5-yl)-1*H*-pyrrol-1-yl)-2-methoxy-*N*-phenyl-benzenesulfonamide (**1i**): White solid; Yield: 91%, m.p. > 250 ^{o}C; IR (KBr) (ν_{max},cm^{-1}): 3395, 3252 (N–H), 3100 (C–H), 1498 (C=C), 1725, 1634 (C=O), 1344, 1161 (SO_2); ^{1}H NMR (400 MHz, DMSO-d_6) δ (ppm): 2.25 (s, 3H, CH_3), 2.40 (s, 3H, CH_3), 3.91 (s, 3H, OCH_3), 4.49 (s, 1H, CH), 7.00-7.04 (m, 5H, Ar), 7.16-7.25 (m, 6H, Ar), 7.40 (dd, 1H, J_1 = 8.8, J_2 = 2.8 Hz, Ar), 7.51 (d, 1H, *J* = 2.8 Hz, Ar), 10.21 (s, 1H, SO_2NH), 11.05 (s, 2H, NH); ^{13}C NMR (100 MHz, DMSO-d_6) δ (ppm): 14.1, 30.7, 48.5, 57.1, 114.0, 114.7, 119.6, 124.1, 126.6, 128.4, 128.8, 129.3, 129.5, 130.0, 130.2, 130.6, 131.0, 135.6, 136.6, 137.0, 138.0, 151.8, 156.4, 169.8, and 194.6; Mass spectrum *m/z*: 586.6 [M^+]; Anal. Calcd. (%) $C_{30}H_{26}N_4O_7S$: C, 61.42; H, 4.47; N, 9.55; S, 5.47; Found: C, 61.11; H, 4.50, N, 4.32; S, 5.19.

3. Results and Discussion

3.1. Chemistry

The synthetic route to obtain pyrrole compounds bearing sulfonamide groups (**1a-i**) is outlined in Scheme 1. Initially, sulfonamide derivatives (**6a-c**) have been carried out according to the reported procedure [43, 44].

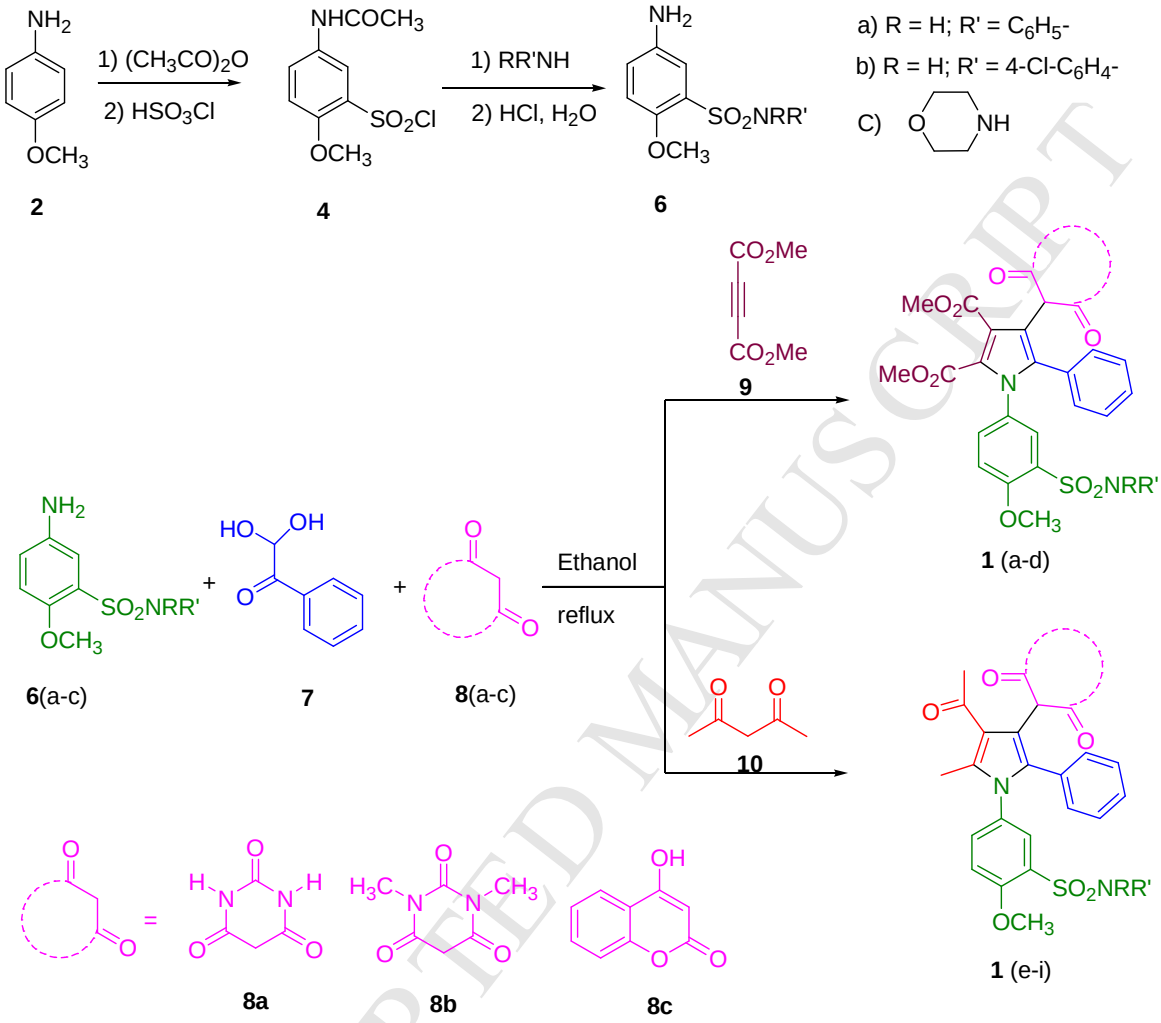

Scheme 1 Synthesis of pyrrole derivatives bearing sulfonamide groups **1a-i**

As demonstrated in Scheme 1, *N*-(4-methoxyphenyl)acetamide **3** was obtained *via* the reaction between *p*-anisidine **2** and acetic anhydride which was treated with chlorosulfonic acid to give the intermediate **4**. The arylsulfonyl chloride intermediate **4** was converted into corresponding sulfonamide **5** in the presence of various amines and anhydrous $NaHCO_3$ at room temperature and under solvent-free conditions. Finally, the compounds (**5a-c**) were hydrolyzed with water and acid to give sulfonamide derivatives (**6a-c**) in high yield and purity. The reaction of sulfonamide derivatives (**6a-c**) with acetylacetone or dimethyl acetylene dicarboxylate, 1, 3-dicarbonyl compounds and phenylglyoxal monohydrate under catalyst-free conditions afforded corresponding final compounds **1a-i** (Scheme 2).

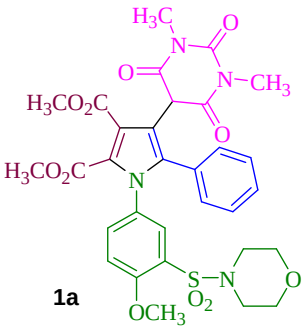

1a

Time = 30 min; Yield = 95%
Amine = **6c** and Dicarbonyl **8b**

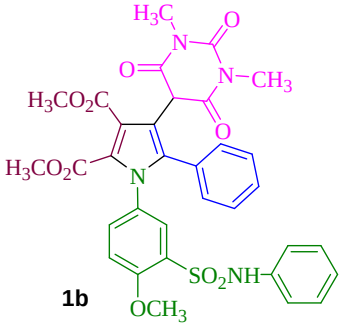

1b

Time = 30 min; Yield = 96%
Amine = **6a** and Dicarbonyl **8b**

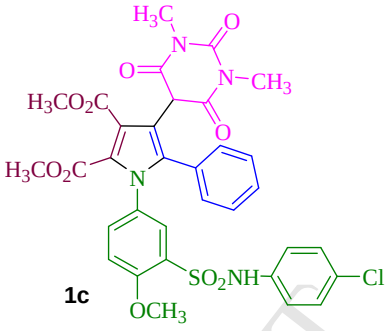

1c

Time = 30 min; Yield = 93%
Amine = **6b** and Dicarbonyl **8b**

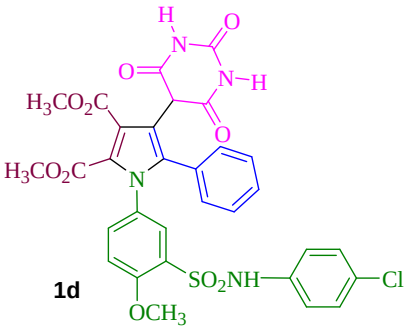

1d

Time = 120 min; Yield = 88%
Amine = **6b** and Dicarbonyl **8a**

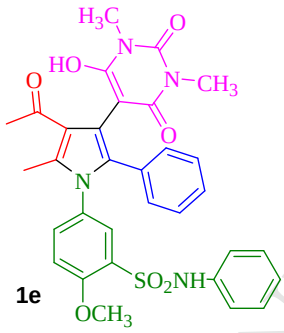

1e

Time = 30 min; Yield = 94%
Amine = **6a** and Dicarbonyl **8b**

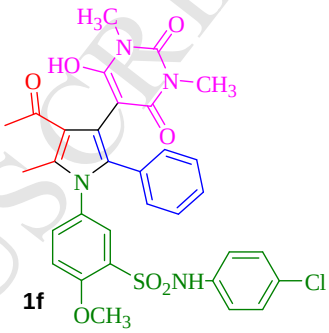

1f

Time = 30 min; Yield = 89%
Amine = **6b** and Dicarbonyl **8b**

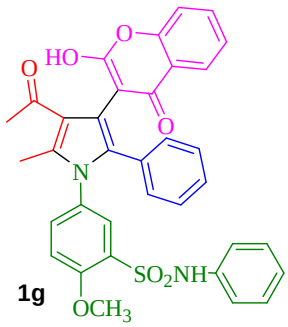

1g

Time = 120 min; Yield = 83%
Amine = **6a** and Dicarbonyl **8c**

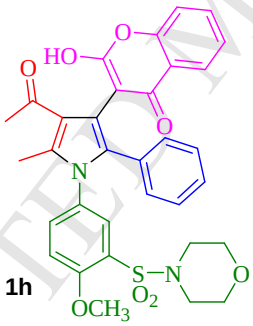

1h

Time = 120 min; Yield = 85%
Amine = **6c** and Dicarbonyl **8c**

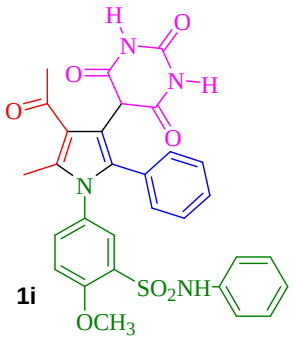

1i

Time = 50 min; Yield = 91%
Amine = **6a** and Dicarbonyl **8a**

Scheme 2 The structure of synthesized pyrrole derivatives bearing sulfonamide groups **1a-i**

High chemical yields were achieved in short reaction time and without the need for column chromatography or recrystallization. It is worth mentioning, there are possible tautomeric structures (Scheme 3) for the synthesized pyrroles. These tautomeric structures come from common hydrogen bonding interaction between hydrogen and oxygen or nitrogen [45, 46]. The structures of these pyrrole derivatives were elucidated on the running spectral data and elemental analysis. The IR spectra of synthesized pyrroles **1a-i** approved clearly the certain structures by observing the absorption bands for C=O, NH, and SO_2 functions at their determined regions. The ^{1}H NMR spectra of pyrroles **1a-c** were shown the singlet peaks at 3.18 ppm and in the region of 3.56-3.90 ppm for the methyl and methoxy protons

respectively. The CH proton of the pyrimidine ring was appeared as singlet between 4.97 and 4.98 ppm. Also, the aromatic protons and the NH proton of the sulfonamide moiety were observed in the region of 6.99-7.68 ppm and 10.21-10.36 ppm, respectively. The ^{13}C NMR spectra of these pyrroles were appeared signals between 152.1 and 168.0 ppm corresponding to the carbonyl carbon atoms and signals between 113.2 and 138.6 ppm corresponding to the carbon–carbon double bonds. Also, aliphatic carbon atoms were shown in the range of 28.9-66.1 ppm.

Similarly, the structures of other pyrrole derivatives were determined by IR, ^{1}H NMR, ^{13}C NMR, Mass spectroscopy and elemental analysis.

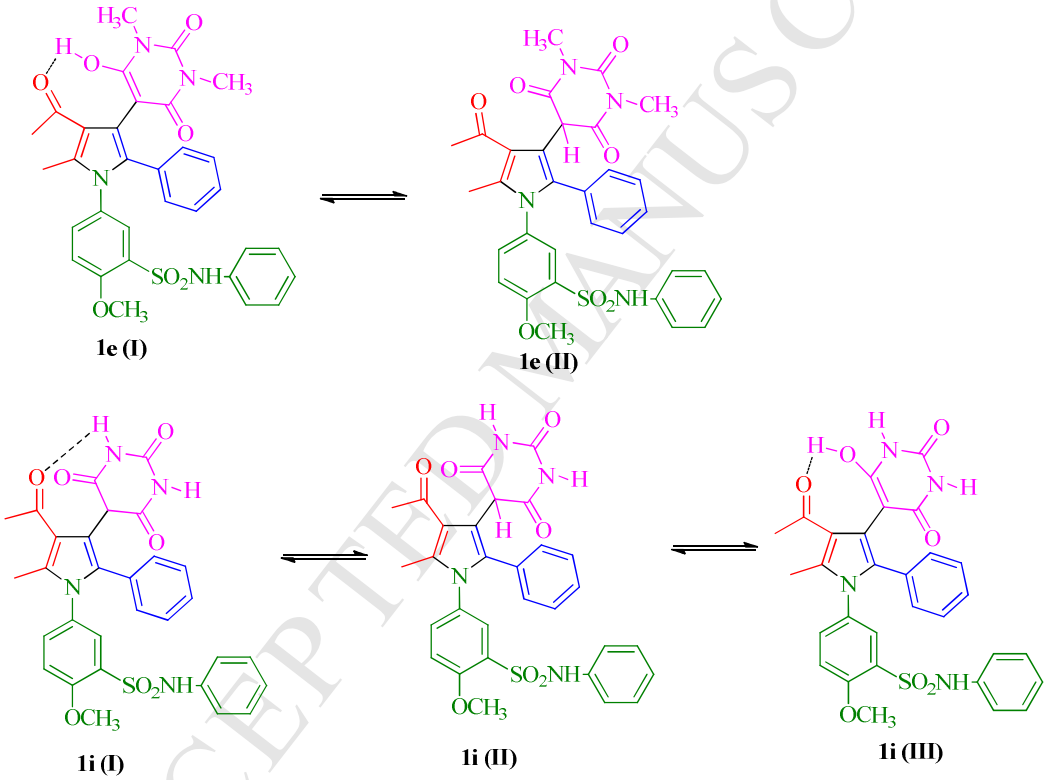

Scheme 3 Possible tautomeric forms of compounds **1e** and **1i**.

3.2. Cytotoxicity activities

All of these new synthesized pyrrole derivatives were screened for biological properties as anticancer activity against three human cell lines including MCF7, MOLT-4 and HL-60 using MTT assay [47]. The different concentrations of the target compounds (25, 50, 100 and 200 µM) was selected to treat with cells and Cisplatin was used as reference drug. The cytotoxicity activity of these analogs is shown in Table 1. The results of tested pyrroles displayed a broad range of cell growth inhibitory activity toward tested cell

lines. Among the compounds **1a-i**, compound **1a** having morpholine ring at sulfonamide moiety exhibited good inhibitory activity against tested cell lines with 39.0, 25.5 and 30.6 µM IC_{50} values for MCF7, MOLT-4 and HL-60 respectively. Replacing morpholine ring (in compound **1a**) with phenyl ring (compound **1b**) at sulfonamide moiety led to loss of inhibitory activity Introduction of chloro substitution to sulfonamide in compound **1c** afforded better inhibitory activity (IC_{50} = 51.2, 38.3 and 45.4 µM respectively) in comparison to its counterpart **1b**. In contrast, the replacement of 1,3-dimethyl barbituric acid group (compound **1c**) with barbituric acid group (compound **1d**) at 4-position of pyrrole ring did not affect inhibitory activity.

Table 1 Cell growth inhibitory activity of synthetic pyrrole derivatives assessed by the MTT reduction assay

Compound	IC_{50} (µM)[a]		
	MCF7	MOLT-4	HL-60
1a	39.0 ± 4.5	25.5 ± 1.1	30.6 ± 3.6
1b	>200	105.5 ± 3.4	95.2± 3.1
1c	51.2 ± 6.2	38.3 ± 5.1	45.4 ± 8.5
1d	61.9 ± 2.6	42.8 ± 3.4	48.1± 5.0
1e	>200	>200	>200
1f	101± 8.1	85.3± 7.6	80.1± 2.7
1g	82.1 ± 6.2	63.2± 2.1	60.3 ± 2.2
1h	65.0± 2.1	40.2± 9.0	42.0± 8.1
1i	123.0 ± 13.6	73.2± 1.3	87.0 ± 4.6
Cisplatin	15.1 ± 0.5	6.3 ± 1.5	8.1 ± 1.3

[a]Values represent mean ± S.E.M.

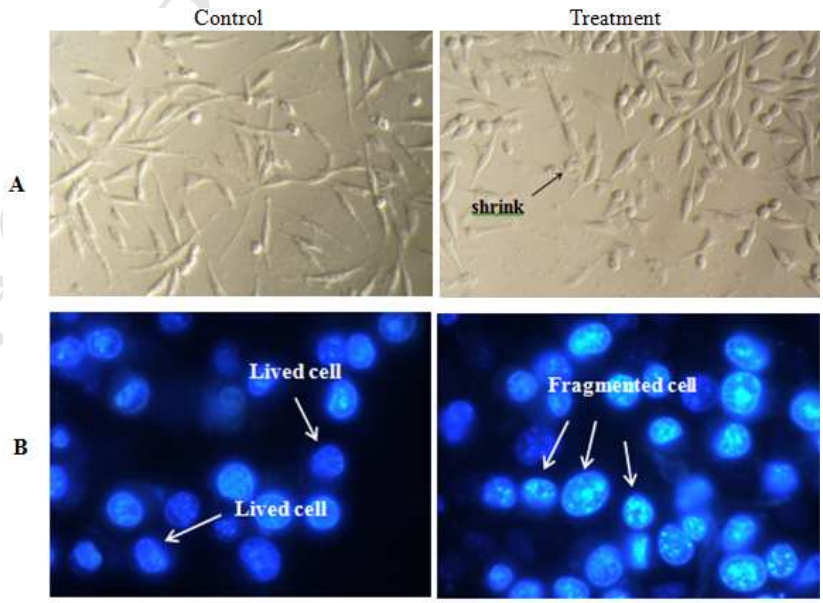

Fig. 4. Morphological analysis of PC-12 cells in the absence and the presence of pyrrole **1a** for 48 h. (A) phase-contrast microscopic images. (B) Fluorescence microscopic images by Hoechst 33258 staining method.

Comparison of IC_{50} value of **1f** with those of unsubstituted analog **1e** showed that insertion of chloro group into 4-phenyl ring of sulfonamide moiety could improve cytotoxic effect. Moreover, compound **1h** having morpholine and coumarin groups at sulfonamide moiety and 4-position of pyrrole ring exhibited inhibitory activity in target cell lines comparing with compound **1g**. It indicated that the introduction of morpholine ring to sulfonamide moiety have better anticancer activity.

After determination of the cytotoxicity of the synthesized compounds, the morphological changes in the nuclei of PC-12 cells were examined using phase-contrast microscopy in the absence and presence of the active compound **1a**. As shown in Fig. 4A, compound **1a**-treated cells lost their polyhedral shape and became shrinking in comparison to control cells. For apoptotic detection, PC-12 cells were stained with Hoechst 33258. As depicted in Fig. 4B, control or untreated cells appeared regular nuclei without any fragmentation. In contrast, the active compound **1a**-exposed cells exhibited chromatin condensation and nuclear fragmentation. Morphological results revealed that the compound **1a** reduced cell viability and induced apoptosis in PC-12 cells.

3.3. Molecular docking study

To better understanding the mechanism of anticancer activity, docking studies were performed to fit pyrrole compounds bearing sulfonamide groups into the active site of FGFR1 (PDB code: 4ZSA) using AutoDock 4.2. The docking results are shown in Table 2. These results exhibited that most of the tested pyrroles displayed hydrogen bonding and hydrophobic interactions with residues present in the active site of target protein. The binding mode of the active compound **1a** with FGFR1 protein is depicted in Fig. 5. In the binding mode, compound **1a** was nicely bound to the active site of the FGFR1 protein by seven hydrogen bonds with Ala564, Lys566, Gly485, Ser565, Arg576 and Tyr563 and hydrophobic interactions with amino acid groups present in the active site which could be contributed to the affinity of compound **1a** with FGFR1. Molecular docking results agreed with the biological assay data, indicated that compound **1a** is possible inhibitor of FGFR1 protein.

Table 2 Molecular docking results of the synthesized compounds with FGFR1

Compound	ΔG (kcal/mol)	H-bonds	
		Amino acids	Distance (Å)
1a	-8.91	Ala564, Lys566, Gly485, Ser565, Arg576 and Tyr563	3.1, 2.8, 2.8, 2.7, 3.0, 3.3 (and 3.5)
1b	-7.82	Glu571, Asn568, Ser565, Tyr563, Lys482	3.5, 2.7, 2.8, 2.9, 3.5
1c	-8.63	Lys482, Gly485, Glu486, Asn568	3.0, 2.7, 2.8, 3.0
1d	-8.12	Asn568, Gly485, Glu486, Pro483, Lys482	3.0, 3.0, 2.8, 3.8, 3.0
1e	-7.35	Ser565, Tyr563, Glu486,	3.0, 2.8, 3.3
1f	-7.95	Asn568	2.7
1g	-8.51	Gly567	2.9
1h	-8.24	Glu571, Gly567	3.3, 2.9
1i	-8.08	Asn568, Glu571	2.6, 3.5

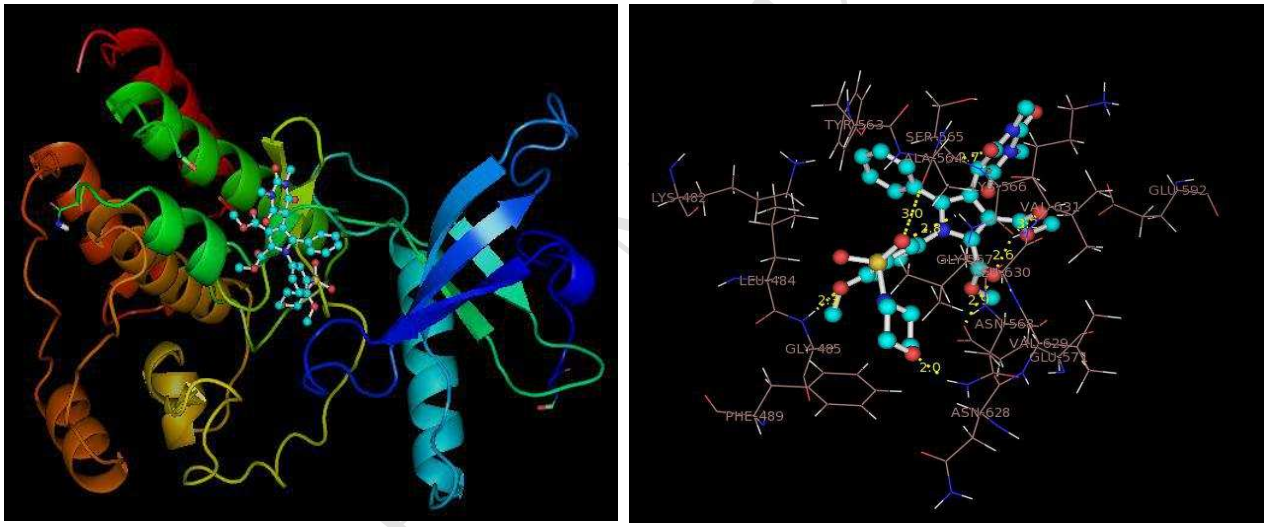

Fig. 5. Presentation of the binding mode for **1a** as the most active compound in the active site of FGFR1 (PDB code: 4ZSA).

3.4. Computations

All calculations were performed with the Gaussian 09 program package [48]. The geometry of compound **1a** was fully optimized without imposing any symmetry constraint with the Becke's three-parameter hybrid functional with the Lee– Yang–Parr correlation functional (B3LYP) [49–51]. The 6-31G (d,p) [52] was employed for the atoms of **1a** [53]. The optimized structure of **1a** was showed in labeled Fig. 6. Frequency was calculated at DFT level, scaled and compared with the experimental frequency to check whether stationary points from the geometry optimization calculations were in real minima. As shown in Table 3,

the calculated bond lengths and bond angles at the level of theory are in reasonable agreement with the crystallographic data.

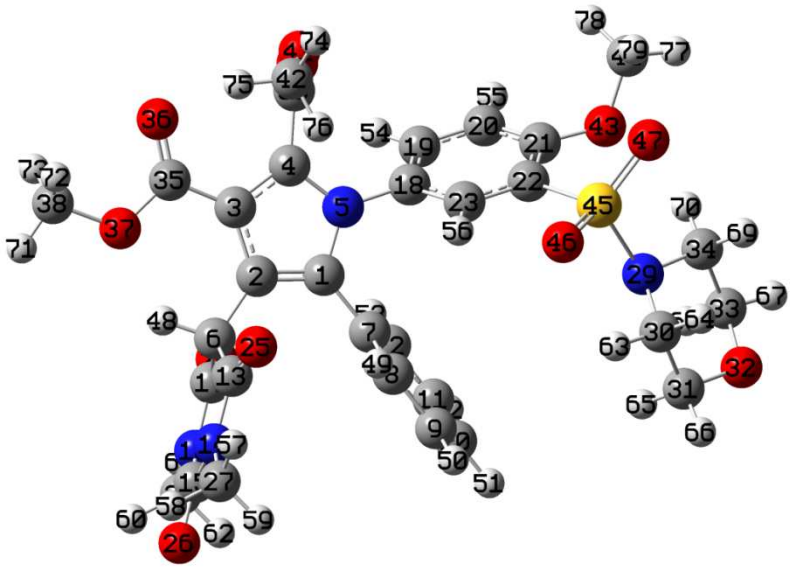

Fig. 6. Optimized structure of compound **1a**

Table 3 Some selected bond lengths (Å) and bond angles (º) of compound **1a** and the experimental data

Bond length (Å)	Calculated	Experimental [a]
C=C (aromatic)	1.39	1.37–1.38
N_5–C_1	1.41	1.41–1.46
C=O (ester)	1.23	1.257-1.287
C=O (amide)	1.24	1.257-1.287
S_{45}–N_{29}	1.88	1.613-1.657
S_{45}=O_{46}, S_{45}=O_{47}	1.64	1.428-1.439
Bond angles (º)		
O_{46}–S_{45}–O_{47}	118.82	118.86
C_{22}–S_{45}–N_{29}	102.61	107.77
O_{46}–S_{45}–C_{22}	105.39	108.05
C_1=C_2–C_6	125.61	121.69–121.67
C_{21}–C_{22}–S_{45}	121.5	120.8
C_{19}–C_{18}–C_{23}	120.32	120.25
O_{36}–C_{35}–C_3	124.85	125.6

C_{35}–O_{37}–C_{38}	116.20	117.5

[a] Ref. [54-61].

^{1}H and ^{13}C NMR in DMSO were calculated with GIAO [62, 63]. IR, ^{1}H NMR and ^{13}C NMR chemical shifts calculated at the B3LYP /6-31+G (d,p) level basis set and compared with experimental data.

An important parameter to measure reactivity of the molecules is the energy gap, ΔE (ΔE = E_{LUMO}–E_{HOMO}). Decreasing in ΔE of the molecule leads to decrease the required energy to remove an electron from the last occupied orbital. A molecule with a low energy gap is usually more polarisable with high chemical activity, low kinetic stability and high softness value [64]. Fig. 7 shows the 3D plots of HOMO and LUMO orbitals of the compound **1a** and gap energy.

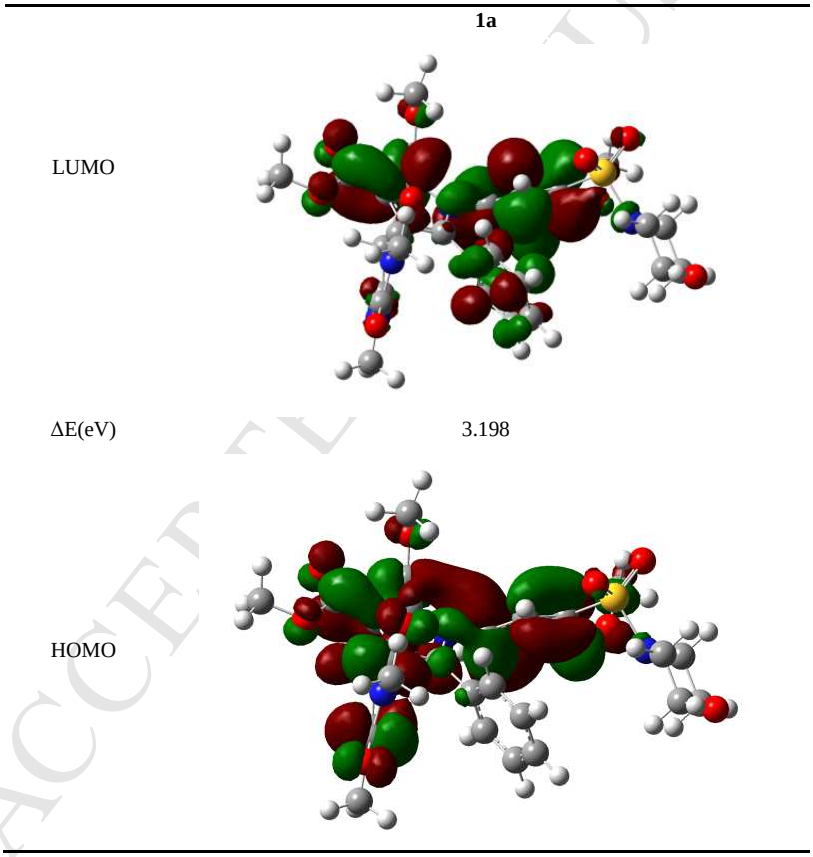

Fig. 7. 3D plots of the HOMO, LUMO orbitals of compound **1a** and ΔE (The enery gap between HOMO and LUMO) (eV)

In addition, DFT is very useful in providing chemical descriptors such as chemical hardness (η), electronegativity (χ), softness (S) and electrophilicity index (ω) Zhou & Navangul (1990) reported the

principle of maximum hardness (absolute hardness) η, for an N-electron system with total energy E and η are defined as:

$$\eta = \left(\frac{\delta^2 E}{\delta N^2}\right) = \frac{1}{2}(IE - EA) = \frac{1}{2}(E_{LUMO}\text{-}E_{HOMO}) \qquad (1)$$

In the formula IE is the vertical ionization energy which is approximated as $-E_{HOMO}$ and EA for the vertical electron affinity as $-E_{LUMO}$ [65]. The global softness is the inverse of chemical hardness ($S=\frac{1}{\eta}$). The electron affinity can also be used in combination with ionization energy to give electronic chemical potential μ, negative of electron affinity ($-\chi$) defined as the characteristic of electronegativity of molecules [66]:

$$\chi = -\mu = \left(\frac{\delta E}{\delta N}\right) = \frac{1}{2}(IE + EA) = -\frac{1}{2}(E_{LUMO}+E_{HOMO}) \qquad (2)$$

The global electrophilicity index, ω, is calculated using the electronic chemical potential μ and chemical hardness η [67]. According to the definition this index measures the propensity of a species to accept electrons and is defined as:

$$S = \frac{\mu^2}{2\eta} \qquad (3)$$

Table 4 shows the gap energy, electronegativity, electrophilicity index and chemical hardness and softness values of the compound **1a.**

Table 4 HOMO–LUMO gap energy, electronegativity, electrophilicity index and chemical hardness and softness values of compound **1a**

1a	
E_{HOMO} (ev)	-7.898
E_{LUMO} (ev)	-4.699
$\Delta E_{L\text{-}H}$ (ev)	3.198
Electronegativity (χ) (ev)	6.299
hardness (η) (ev)	1.599
Softness (S) (ev^{-})	0.3126
Electrophilicity (ψ) (ev)	12.405

3.4.1. Computational IR

Infrared spectra were recorded on KBr Pellet and the vibrational frequencies of **1a** were calculated at the B3LYP / 6-31G+(d,p) level of theory. In order to assign the calculated frequency to the approximate vibrational descriptor, the vibration modes have been analyzed by means of atom movements, calculated in Cartesian coordinates. The observed and calculated vibration frequencies of the compound in the 3200–400 cm^{-1} region were summarized in Table 5.

The observed bands at 2980.7 and 2850.4 cm^{-1} are assigned to CH stretching vibrations in aliphatic moieties. The calculated wave numbers corresponding to these bands are found at 3014.4 and 2857.5 cm^{-1} respectively. The CH in-plane bending vibrations can be occurred in the region 1600–1000 $cm^{-1}$and are mostly observed as combined with other vibrational modes. For example, the observed bands at 1165.0, 1202.0, 1451.7 and 1493.0 cm^{-1} including in plane bending modes are uncovered as mixed with vibrational modes such as ν_{CC} in ring and ν_{CCC} in ring. The CH out-of-plane bending vibrations are observed at the interval 1000–650 cm^{-1} [68–72]. In this study, the observed bands 1016.6-760.6 cm^{-1} is assigned to the CH out-of-plane bending modes which were computed at 985.2-770.8 cm^{-1}. The asymmetric and symmetric stretching vibration of SO_2 were appeared at 1381.7-1275.7 while were calculated at 1386.4-1276.5 respectively.

Table 5 Experimental and scaled vibrational wavenumbers (harmonic frequency) (cm^{-1}), and assignments of **1a** utilizing (6-31G+ (d,p) basis set

1a		Assignment
Exprimental	Scaled	
2980.7	3014.4	ν (C-H) Aliphatic(asymmetric)
2850.4	2857.5	ν (C-H) Aliphatic(symmetric)
1710.1	1729.7	ν (C=O)
1677.4	1678.2	ν (C=O)
1522.3	1577.7	ν (C=C)
1493.0	1502.4	βHCC
1451.7	1405.4	βHCC
1381.7	1386.4	SO_2(asym)
1275.7	1276.5	SO_2(sym)
1202.0	1215.6	βHCC
1165.0	1162.3	βHCC
1016.6	985.2	ɣCH
950.6	963.2	ɣCH
760.6	770.8	ɣCH
740.3	764.3	SO_2(scis)

3.4.2. Computational NMR

The isotropic chemical shifts are frequently used as an aid in identification of organic compounds and accurate predictions of molecular geometries are essential for reliable studies of magnetic properties. The ^{13}C and ^{1}H NMR isotropic shielding were calculated with the GIAO method [73, 74] using the optimized parameters obtained from B3LYP by /6-31+G (d,p) methods. The GIAO method is one of the most common approaches for calculating nuclear magnetic shielding tensors. In order to comparison between experimental and theoretical NMR data, this may be helpful in making correct assignments and understanding the relationship between chemical shift and molecular structure. ^{13}C NMR chemical shifts calculation for further clarification of the synthesized complexes is reported. To clarify the relation between theoretical and experimental values of NMR chemical shift constants, the experimental data are plotted versus computed values. The impact of the solvent was taken into account using the Polarized Continuum Model (PCM) [75]. In order to compute the ^{13}C NMR chemical shifts, each couple of carbon atoms on equivalent locations of the compound were considered as equivalent and their average of chemical shifts were calculated. The isotropic ^{1}H and ^{13}C chemical shifts calculated by all DFT methods are given in Table 6, 7 respectively and compared with the experimental values. As can be seen, the results obtained by using all methods are in reasonable agreement with experimental values. The chemical shift changes with methods presumably occur due to variation of the hybrid functional. The results of B3LYP method are close to experimental data and they differ slightly from results of experiment. As can be seen, there is a good linear relationship between experimental and theoretical B3LYP/6-31+G (d,p) chemical shifts (for more details see SI, Fig. 30 and 31).

Table 6 The Experimental and calculated ^{1}H NMR nuclear shielding and assignments of **1a** utilizing basis sets 6-31G+ (d,p)

	1a	
Experimental	6-31+G(d,p)	Assignment
7.36	8.04	54
7.68	7.17	56
7.34	7.06	49
7.27	6.96	50
7.18	6.87	55
7.32	6.69	53
4.98	6.25	48
3.90	4.32	75
3.69	3.88	72,73
3.18	3.70	61
3.64	3.52	78
2.78	3.41	63
2.78	3.31	69
3.52	3.19	65
3.14	2.87	58

$R^2 = 0.971$ (R = root-mean-square deviation)

Table 7 The Experimental and calculated ^{13}C NMR nuclear shielding and assignments of **1a** utilizing basis sets 6-31G+ (d,p)

Experimental	6-31+G(d, p)	Assignment
168.00	175.87	C13
163.89	173.71	C35
157.04	158.08	C21
152.15	155.29	C15
138.74	142.66	C1
131.06	139.37	C19
129.74	136.02	C4
134.78	135.48	C18
130.72	133.84	C8
131.06	132.54	C7
129.32	129.56	C11
129.16	129.48	C10
128.89	129.08	C9
114.27	128.80	C23
113.52	127.40	C20
128.36	123.42	C3
124.75	123.09	C2
66.09	76.52	C31
66.09	75.30	C33
56.96	73.24	C44
53.34	58.92	C38

48.16	58.06	C6
46.11	56.17	C30
28.90	35.05	C27
28.90	34.72	C28

R^2 = 0.986 (R = root-mean-square deviation)

4. Conclusions

In conclusion, a new set of pyrrole derivatives bearing sulfonamide groups was synthesized and characterized using various spectroscopic techniques. The synthesized pyrrole derivatives were evaluated for their toxicity against MCF7, MOLT-4 and HL-60 cell lines. Among them, compound **1a** possessing morpholine ring at sulfonamide moiety displayed good inhibitory activity. The morphological analysis by Hoechst 33258 staining test demonstrated that the active compound **1a** can induce apoptosis in PC-12 cells. Also, Molecular docking studies were performed to insert these compounds into FGFR1 active site to predict a possible binding mode. The obtained results suggested that compound **1a** may be a promising lead for further modifications towards search of potent antineoplastic agents. In addition, DFT calculations were used successfully to optimize the structural of compound **1a** and support the IR and NMR data.

Acknowledgment:

We are thankful to Persian Gulf University Research Council for partial support of this work.

References:

[1] T. Nasr, S. Bondock, M. Youns, Anticancer activity of new coumarin substituted hydrazide–hydrazone derivatives, Eur. J. Med. Chem. 76 (2014) 539-548.

[2] K.H. Tiong, L.Y. Mah, C.O. Leong, Functional Roles of Fibroblast Growth Factor Receptors (FGFRs) Signaling in Human Cancers, Apoptosis. 18 (2013) 1447-1468.

[3] A.N. Brooks, E. Kilgour, P.D. Smith, Molecular Pathways: Fibroblast Growth Factor Signaling: A New Therapeutic Opportunity in Cancer, Clinical Cancer Research. 18 (2012) 1855-1862.

[4] R.T. Bottcher, C. Niehrs, Fibroblast growth factor signaling during early vertebrate development, Endocr Rev. 26 (2005) 63-77.

[5] M. Katoh, FGFR inhibitors: Effects on cancer cells, tumor microenvironment and whole-body homeostasis (Review), Int. J. Mol. Med. 38 (2016) 3-15.

[6] Y.K. Chae, K. Ranganath, P.S. Hammerman, C. Vaklavas, N. Mohindra, A. Kalyan, M. Matsangou, R. Costa, B. Carneiro, V.M. Villaflor, M. Cristofanilli. F.J. Giles, Inhibition of the fibroblast growth factor receptor (FGFR) pathway: the current landscape and barriers to clinical application, Oncotarget. 8 (2017) 16052-16074.

[7] C. Peifer, R. Selig, K. Kinkel, D. Ott, F. Totzke, C. Schächtele, R. Heidenreich, M. Röcken, D. Schollmeyer, S. Laufer, Design, Synthesis, and Biological Evaluation of Novel 3-Aryl-4-(1*H*-indole-3yl)-1,5-dihydro-2*H*-pyrrole-2-ones as Vascular Endothelial Growth Factor Receptor (VEGF-R) Inhibitors, J. Med. Chem. 51 (2008) 3814-3824.

[8] Z. Chen, X. Wang, W. Zhu, X. Cao, L. Tong, H. Li, H. Xie, Y. Xu, S. Tan, D. Kuang, J. Ding, X. Qian, Acenaphtho[1,2-*b*]pyrrole-Based Selective Fibroblast Growth Factor Receptors 1 (FGFR1) Inhibitors: Design, Synthesis, and Biological Activity, J. Med. Chem. 54 (2011) 3732-3745.

[9] J. Liu, X. Peng, Y. Dai, W. Zhang, S. Ren, J. Ai, M. Geng, Y. Li, Design, synthesis and biological evaluation of novel FGFR inhibitors bearing an indazole scaffold, Org. Biomol. Chem. 13 (2015) 7643-7654.

[10] S.S. Gholap, Pyrrole: An emerging scaffold for construction of valuable therapeutic agents, Eur. J. Med. Chem. 110 (2016) 13-31.

[11] H. Fan, J. Peng, M.T. Hamann, J.F. Hu, Lamellarins and Related Pyrrole-Derived Alkaloids from Marine Organisms, Chem. Rev. 108 (2008) 264-287.

[12] R.W. Burli, D. McMinn, J.A. Kaizerman, W. Hu, Y. Ge, Q. Pack, V. Jiang, M. Gross, M. Gracia, R. Tanaka, H.E. Moser, DNA binding ligands targeting drug-resistant Gram-positive bacteria. Part 1: Internal benzimidazole derivatives, Bioorg. Med. Chem. Lett. 14 (2004) 1253-1257.

[13] S.D. Joshi, S.R. Dixit, M.N. Kirankumar, T.M. Aminabhavi, K.V.S.N. Raju, R. Narayan, C. Lherbet, K.S. Yang, Synthesis, antimycobacterial screening and ligand-based molecular docking studies on novel pyrrole derivatives bearing pyrazoline, isoxazole and phenyl thiourea moieties, Eur. J. Med. Chem. 107 (2016) 133-152.

[14] A. Kamal, G. Ramakrishna, V. Lakshma Nayak, P. Raju, A.V. Subba Rao, A. Viswanath, M.V. Vishnuvardhan, S. Ramakrishna, G. Srinivas, Design and synthesis of benzo[*c,d*]indolone-pyrrolobenzodiazepine conjugates as potential anticancer agents, Bioorg. Med. Chem. 20 (2012) 789-800.

[15] C. Battilocchio, G. Poce, S. Alfonso, G.C. Porretta, S. Consalvi, L. Sautebin, S. Pace, A. Rossi, C. Ghelardini, L.D. Cesare Mannelli, S. Schenone, A. Giordani, L.D. Francesco, P. Patrignani, M. Biava, A class of pyrrole derivatives endowed with analgesic/anti-inflammatory activity, Bioorg. Med. Chem. 21 (2013) 3695-3701.

[16] M.N. Narule, M.K. Gaidhane, P.K. Gaidhane, Synthesis, characterization, biologically and antioxidant active of some 2-substituted3, 5- dimethyl- 4-ethoxy carbonyl pyrrole derivatives, J. Pharm. Res. 6 (2013) 626-632.

[17] V. Estévez, M. Villacampa, J.C. Menéndez, Multicomponent reactions for the synthesis of pyrroles, Chem. Soc. Rev. 39 (2010) 4402-4421.

[18] E. Fernandes, D. Costa, S.A. Toste, L.F.C. Lima, S. Reis, In vitro scavenging activity for reactive oxygen and nitrogen species by nonsteroidal anti-inflammatory indole, pyrrole, and oxazole derivative drugs, Free Radic Biol. Med. 37 (2004) 1895-1905.

[19] M. Biaya, G.C. Porretta, G. Poce, A. De Logu, R. Meleddu, E. De Rossi, F. Manetti, M. Botta, 1,5-Diaryl-2-ethyl pyrrole derivatives as antimycobacterial agents: Design, synthesis, and microbiological evaluation, Eur. J. Med. Chem. 44 (2009) 4734-4738.

[20] M. Biava, G.C. Porretta, G. Poce, S. Supino, D. Deidda, R. Pompei, P. Molicotti, F. Manetti, M. Botta, Antimycobacterial agents. Novel diarylpyrrole derivatives of BM212 endowed with high activity toward Mycobacterium tuberculosis and low cytotoxicity, J. Med. Chem. 49 (2006) 4946-4952.

[21] Z. Ye, L. Shi, X. Shao, X. Xu, Z. Li, Pyrrole- and Dihydropyrrole-Fused Neonicotinoids: Design, Synthesis, and Insecticidal Evaluation, J. Agric. Food. Chem. 61 (2013) 312-319.

[22] S. Pu, G. Liu, L. Shen, J. Xu, Efficient Synthesis and Properties of Isomeric Photochromic Diarylethenes Having a Pyrrole Unit, Org. Lett. 9 (2007) 2139-2142.

[23] S.J. Higgins, Conjugated polymers incorporating pendant functional groups-synthesis and characterization, Chem. Soc. Rev. 26 (1997) 247-257.

[24] M.M. Ghorab, F.A. Ragab, H.I. Heiba, M.G. El-Gazzar, S.S. Zahran, Synthesis, anticancer and radiosensitizing evaluation of some novel sulfonamide derivatives, Eur. J. Med. Chem. 92 (2015) 682-692.

[25] N. Boechat, L.C.S. Pinheiro, O.A. Santos-Filho, I. C. Silva, Design and Synthesis of New *N*-(5-Trifluoromethyl)-1*H*-1,2,4-triazol-3-yl Benzenesulfonamides as Possible Antimalarial Prototypes. Molecules, 16 (2011) 8083-8097.

[26] I.R. Greig, E. Coste, S.H. Ralston, R.J. van't Hof, Development of triarylsulfonamides as novel anti-inflammatory agents, Bioorg. Med. Chem. Lett. 23 (2013) 816-820.

[27] M. Banerjee, A. Poddar, G. Mitra, A. Surolia, T. Owa, B. Bhattacharyya, Sulfonamide Drugs Binding to the Colchicine Site of Tubulin: Thermodynamic Analysis of the Drug−Tubulin Interactions by Isothermal Titration Calorimetry, J. Med. Chem. 48 (2005) 547-555.

[28] Z. Chen, W. Xu, K. Liu, S. Yang, H. Fan, P.S. Bhadury, D.Y. Hu, Y. Zhang, Synthesis and Antiviral Activity of 5-(4-Chlorophenyl)-1,3,4-Thiadiazole Sulfonamides, Molecules. 15 (2010) 9046-9056.

[29] A. Scozzafava, T. Owa, A. Mastrolorenzo, C.T. Supuran, Anticancer and antiviral sulfonamides, Curr. Med. Chem. 10 (2003) 925-953.

[30] M. Jiyoung, A.J Adnan, S.D Narra, L. Yuan, G.V.M Erwin, M.G Mark, Structure–activity relationship of 2,2-dimethyl-*2H*-chromene based arylsulfonamide analogs of 3,4-dimethoxy-*N*-[(2,2-dimethyl-2*H*-chromen-6-yl)methyl]-*N*-phenylbenzenesulfonamide, a novel small molecule hypoxia inducible factor-1 (HIF-1) pathway inhibitor and anti-cancer agent, Bioorg. Med. Chem 20 (2012) 4590-4597.

[31] G.M. Brown, The biosynthesis of pteridines, Adv. Enzymol. Relat. Areas Mol. Biol. 35 (1971) 35-77.

[32] X.C. Cheng, Q. Wang, H. Fang, W.F. Xu, Role of Sulfonamide Group in Matrix Metalloproteinase Inhibitors, Curr. Med. Chem. 15 (2008) 368-373.

[33] E. Barresi, S. Salerno, A.M. Marini, S. Taliani, C.L. Motta, F. Simorini, F.D. Settimo, D. Vullo, C.T. Supuran, Sulfonamides incorporating heteropolycyclic scaffolds show potent inhibitory action against carbonic anhydrase isoforms I, II, IX and XII, Bioorg. Med. Chem. 24 (2016) 921-927.

[34] M.J. Walsh, K.R. Brimacombe, H. Veith, J.M. Bougie, T. Daniel, W. Leister, L. C. Cantley, W.J. Israelsen, M.G.V. Heiden, M. Shen, D.S. Auld, C.J. Thomas, M.B. Boxer, 2-Oxo-*N*-aryl-1,2,3,4-tetrahydroquinoline-6-sulfonamides as activators of the tumor cell specific M2 isoform of pyruvate kinase, Bioorg. Med. Chem. Lett. 21 (2011) 6322-6327.

[35] T. Owa, H. Yoshino, T. Okauchi, K. Yoshimatsu, Y. Ozawa, N.H. Sugi, T. Nagasu, N. Koyanagi, K. Kitoh, Discovery of Novel Antitumor Sulfonamides Targeting G1 Phase of the Cell Cycle, J. Med. Chem. 42 (1999) 3789-3799.

[36] C.T. Supuran, Carbonic anhydrase inhibitors and activators for novel therapeutic applications, Future Med. Chem. 3 (2011) 1165-80.

[37] C.T. Supuran, A. Scozzafava, Carbonic Anhydrase Inhibitors, Cur. Med. Chem. Imm. Endoc. Metab. Agent. 1 (2001) 61-97.

[38] C.T. Supuran, A. Scozzafava, Carbonic anhydrase inhibitors and their therapeutic potential, Exp Opin. Ther. Pat. 10 (2000) 575-600.

[39] S. Allen, J. Sotos, M.J. Sylte, C.J. Czuprynski, Use of Hoechst 33342 staining to detect apoptotic changes in bovine mononuclear phagocytes infected with Mycobacterium avium subsp. paratuberculosis, Clinical and Diagnostic Laboratory Immunology. 8 (2001) 460-464.

[40] M.M. Word, S.C. Lovell, J.S. Richardson, D.C. Richardson, Asparagine and Glutamine: Using Hydrogen Atom Contacts in the Choice of Side-chain Amide Orientation, J. Mol. Biol. 285 (1999) 1735–1747.

[41] N. Eswar, B. John, N. Mirkovic, A. Fiser, V.A. Ilyin, U. Pieper, A.C. Stuart, M.A. Marti-Renom, M.S. Madhusudhan, B. Yerkovich, Tools for comparative protein structure modeling and analysis, Nucleic Acids Res. 31 (2003) 3375-3380.

[42] Y. Dommaraju, D. Prajapati, A highly efficient group-assisted purification method for the synthesis of poly-functionalized pyrimidin-5-yl-pyrroles via one-pot four-component domino reaction, Mol Divers. 19 (2015) 173-87.

[43] A.R. Massah, D. Azadi, H. Aliyan, A.R. Momeni, H. Javaherian Naghash, F. Kazemi, An Efficient Method for the Synthesis of *N*-Acylsulfonamides: One-pot Sulfonylation and Acylation of Primary Arylamines under Solvent-Free Conditions, Monatsh. Chem. 139 (2008) 233-240.

[44] M. Bavadi, K. Niknam, M. Gharibi, Synthesis of new dihydropyrrol-2-one derivatives bearing sulfonamide groups and studies their antibacterial activity, Monatsh. Chem. (2016) In print. doi: 10.1007/s00706-016-1847-y.

[45] Z.H. Chohan, M.H. Youssoufi, A. Jarrahpour, T. B. Hadda, Identification of antibacterial and antifungal pharmacophore sites for potent bacteria and fungi inhibition: Indolenyl sulfonamide derivatives, Eur. J. Med. Chem. 45 (2010) 1189–1199.

[46] S.S. Sajadikhah, M.T. Maghsoodlou, A simple and green approach for the synthesis of polyfunctionalized mono- and bis-dihydro-2-oxopyrroles catalyzed by trityl chloride, RSC Adv. 4 (2014) 43454-43459.

[47] T. Mosmann, Rapid colorimetric assay for cellular growth and survival: application to proliferation and cytotoxicity assays, J. Immunol. Methods. 65 (1983) 55-63.

[48] M.J. Frisch, G.W. Trucks, H.B. Schlegel, G.E. Scuseria, M.A. Robb, J.R. Cheeseman, J.A. Montgomery, Jr., T. Vreven, K.N. Kudin, J.C. Burant, J.M. Millam, S.S. Iyengar, J. Tomasi, V. Barone, B. Mennucci, M. Cossi, G. Scalmani, N. Rega, G.A. Petersson, H. Nakatsuji, M. Hada, M. Ehara, K. Toyota, R. Fukuda, J. Hasegawa, M. Ishi7€87621da, T. Nakajima, Y. Honda, O. Kitao, H. Nakai, M. Klene, X. Li, J.E. Knox, H.P. Hratchian, J.B. Cross, V. Bakken, C. Adamo, J. Jaramillo, R. Gomperts, R.E. Stratmann, O. Yazyev, A.J. Austin, R. Cammi, C. Pomelli, J.W. Ochterski, P.Y. Ayala, K. Morokuma, G.A. Voth, P. Salvador, J.J. Dannenberg, V.G. Zakrzewski, S. Dapprich, A.D. Daniels, M.C. Strain, O. Farkas, D.K. Malick, A.D. Rabuck, K. Raghavachari, J.B. Foresman, J.V. Ortiz, Q. Cui, A.G. Baboul, S. Clifford, J. Cioslowski, B.B. Stefanov, G. Liu, A. Liashenko, P. Piskorz, I. Komaromi, R.L. Martin, D.J. Fox, T. Keith, M.A. Al-Laham, C.Y. Peng, A. Nanayakkara, M. Challacombe, P.M.W. Gill, B. Johnson, W. Chen, M.W. Wong, C. Gonzalez, J.A. Pople, Gaussian 09, revision C.01, Gaussian Inc., Wallingford CT, 2009.

[49] C. Lee, W. Yang, R.G. Parr, Development of the Colle-Salvetti correlation-energy formula into a functional of the electron density, Phys. Rev. B. 37 (1988) 785–789.

[50] A.D. Becke, Density-functional exchange-energy approximation with correct asymptotic behavior, Phys. Rev. A. 38 (1988) 3098–3100.

[51] A.D. Becke, Density-functional thermochemistry. III. The role of exact exchange, J. Chem. Phys. 98 (1993) 5648–5652.

[52] W.J. Hehre, L. Radom, P.V.R. Schleyer, J. Pople, Ab Initio Molecular Orbital Theory, Wiley & Sons, New York, 1986.

[53] P.J. Hay, W.R. Wadt, Ab initio effective core potentials for molecular calculations. Potentials for K to Au including the outermost core orbitals, J. Chem. Phys. 82 (1985) 299-310.

[54] A. M. Mansour, Selective coordination ability of sulfamethazine Schiff-base ligand towards copper (II): Molecular structures, spectral and SAR study, Spectrochim. Acta, Part A. 123 (2014) 257–266.

[55] R.M. Kuznetsov, A.S. Balueva, I.A. Litvinov, A.T. Gubaidullin, G.N. Nikonov, A.A. Karasik, O.G. Sinyashin, Synthesis of new macrocyclic aminomethylphosphines based on 4,4"-diaminodiphenylmethane and its derivatives, Russ. Chem. Bull. 51(2002) 151–156.

[56] V. Jevtovic, D. Cvetkovic, D. Vidovic, Synthesis, X-Ray Characterization and Antimicrobial Activity of Iron(II) and Cobalt(III) Complexes with the Schiff Base Derived from Pyridoxal and Semicarbazide or S-methylisothiosemicarbazide, J. Iran. Chem. Soc.8 (2011) 727-733.

[57] J.A. Ganaie, J. Kumar, R.J. Butcher, J.P. Jasinski, S.K. Gupta, Synthesis, Crystal Structures and DFT Calculations of Two New Phenol-Based Ester Derivatives, J. Chem. Crystallogr. 46 (2016) 93-104.

[58] K. Sarojini, H. Krishnan, C.C. Kanakam, S. Muthu, Synthesis, X-ray structural, characterization, NBO and HOMO–LUMO analysis using DFT study of 4-methyl-N-(naphthalene-1-yl)benzene sulfonamide, Spectrochim. Acta, Part A. 96 (2012) 657–667.

[59] E.V. Mironova, O.A. Lodochnikova, D.B. Krivolapov, Ya.V. Veremeichik, V.V. Plemenkov, I. A. Litvinov, Crystal structure of cyclic sulfin- and sulfonamides of the thiazine series: conformation, intra- and intermolecular interactions, J. Struct. Chem. 55 (2014) 539-547.

[60] B.T. Loughrey, M.L. Williams, P.C. Healy, 4-(Benzyl-ideneamino) benzene-sulfonamide, Acta Cryst. E65 (2009) o2087–o2096.

[61] G. Grivani, V. Tahmasebi, K. Eskandri, A. D. khalaji, G. Bruno and H. A. Rubari, Synthesis, characterization, crystal structure determination and computational study of the two new bidentate O, N Schiff bases derived from bromosalicylaldehyde and amines containing alkyl halide pendant groups, J. Mol. Struct. 1054-1055 (2013) 100-106.

[62] R. Ditchfield, Molecular Orbital Theory of Magnetic Shielding and Magnetic Susceptibility, J. Chem. Phys. 56 (1972) 5688–5691.

[63] K. Wolinski, J.F. Hinton, P. Pulay, Efficient implementation of the gauge-independent atomic orbital method for NMR chemical shift calculations, J. Am. Chem. Soc. 112 (1990) 8251–8260.

[64] H.G.O. Becker, Jan Fleming, Frontier Orbitals and Organic Chemical Reactions, New York: John Wiley & Sons, 1976.

[65] Z. Zhou, H.V. Navangul, Absolute hardness and aromaticity: MNDO study of benzenoid hydrocarbons, J. Phys. Org. Chem. 3 (1990) 784-788.

[66] T. Koopmans, Über die Zuordnung von Wellenfunktionen und Eigenwerten zu den Einzelnen Elektronen Eines Atoms, Physica. 1 (1934) 104-113.

[67] C. Lee, W. Yang, R.G. Parr, Development of the Colle-Salvetti correlation-energy formula into a functional of the electron density, Phys. Rev. B. 37 (1988) 785-789.

[68] N.B. Colthup, L.H. Daly, E. Wiberley, Introduction to Infrared and Raman Spectroscopy, Academic Press, New York, 1964.

[69] H.H. Perkampus, LJ Bellamy: The Infrared Spectra of Complex Molecules, third ed., Wiley, New York, 1975.

[70] J.B. Lambert, H.F. Shurvell, R.G. Cooks, Introduction to Organic Spectroscopy, Macmillan Publishing, New York, USA, 1987.

[71] B.H. Stuart, Infrared Spectroscopy: Fundamentals and Applications, John Willey & Sons, England, 2004.

[72] D.L. Pavia, G.M. Lampman, G.S. Kriz, J.R. Vyvyan, Introduction to Spectroscopy: A Guide for Students of Organic Chemistry, Brooks/Cole Cengage Learning, USA, 2009.

[73] R. Ditchfield, Molecular Orbital Theory of Magnetic Shielding and Magnetic Susceptibility, J. Chem. Phys. 56 (1972) 5688–5691.

[74] K. Wolinski, J.F. Hinton, P. Pulay, Efficient implementation of the gauge-independent atomic orbital method for NMR chemical shift calculations, J. Am. Chem. Soc. 112 (1990) 8251–8260.

[75] V. Barone, M. Cossi, R. Cammi, J. Tomasi, Ab initio study of solvated molecules: a new implementation of the polarizable continuum model, J. Chem. Phys. Lett. 255 (1996) 327-335.

► A series of novel pyrrole derivatives bearing sulfonamide groups were synthesized and characterized.

► Cytotoxicity of the synthesized pyrroles was evaluated against MCF7, MOLT-4 and HL-60 cell lines.

► Molecular docking studies were performed to determine the probable binding mode of the designed pyrrole derivatives into the active site of FGFR1 protein.

► DFT calculations were performed to optimize the structure of compound **1a** and supported the IR and NMR data.